Liquid Crystals
Publication details, including instructions for authors and subscription information:
http://www.informaworld.com/smpp/title~content=t713926090

Observation of intercalated smectic phases in symmetric liquid crystal dimers containing hydrazide groups

Haitao Wang[a]; Binglian Bai[a]; Peng Zhang[ab]; Beihong Long[a]; Wenjing Tian[b]; Min Li[a]
[a] Key laboratory of Automobile Materials, Ministry of Education, Institute of Materials Science and Engineering, Jilin University, Changchun 130012, PR China [b] Key Laboratory of Supramolecular Structure and Materials, Ministry of Education, Institute of Chemistry, Jilin University, Changchun 130012, PR China

To cite this Article Wang, Haitao , Bai, Binglian , Zhang, Peng , Long, Beihong , Tian, Wenjing and Li, Min(2006) 'Observation of intercalated smectic phases in symmetric liquid crystal dimers containing hydrazide groups', Liquid Crystals, 33: 4, 445 — 450

To link to this Article: DOI: 10.1080/02678290600604841

URL: http://dx.doi.org/10.1080/02678290600604841

Liquid Crystals, Vol. 33, No. 4, April 2006, 445–450

Taylor & Francis
Taylor & Francis Group

Observation of intercalated smectic phases in symmetric liquid crystal dimers containing hydrazide groups

HAITAO WANG†, BINGLIAN BAI†, PENG ZHANG†‡, BEIHONG LONG†, WENJING TIAN‡ and MIN LI*†

†Key laboratory of Automobile Materials, Ministry of Education, Institute of Materials Science and Engineering, Jilin University, Changchun 130012, PR China

‡Key Laboratory of Supramolecular Structure and Materials, Ministry of Education, Institute of Chemistry, Jilin University, Changchun 130012, PR China

(*Received 22 July 2005; in final form 1 December 2005; accepted 20 December 2005*)

Dimeric hydrazide derivatives with nitro, phenyl, and methyl terminal subsistents were synthesized. The liquid crystalline properties were investigated by differential scanning calorimetry, polarizing optical microscopy and wide angle X-ray diffraction. Interestingly, intercalated smectic phases were observed in these symmetric liquid crystal dimers. The effect of the substituents and the length of the spacer on the mesophase is discussed, confirming that intermolecular hydrogen bonding between the hydrazide groups was the driving force for the formation of the intercalated structures.

1. Introduction

Liquid crystal dimers [1] are composed of molecules containing two mesogenic groups linked via a flexible spacer. They can be sub-divided into two broad groups: symmetric dimers, in which the two mesogenic units are identical, and non-symmetric dimers, which contain two different mesogenic units [2, 3]. Initial interest in these materials stemmed from their use as model compounds for semi-flexible main chain liquid crystal polymers [4, 5]; they are now of fundamental interest in their own right due to their unique phase behaviour, and their smectic polymorphism [1–3] which are significantly different from those of conventional low molar mass liquid crystals.

For the majority of symmetric dimers containing terminal alkyl chains, a simple empirical rule has emerged relating the occurrence of smectic behaviour to the molecular structure; specifically, if a symmetric dimer is to exhibit a smectic phase then the terminal chain length must be greater than half the spacer length [1–3, 6]. This empirical rule effectively eliminates the possibility that symmetric dimers form an intercalated structure simply because the terminal chains can only be accommodated within such a structure if the total length of the two terminal chains is equal to or less than that of the spacer [2]. Symmetric dimers appear therefore to have a strong tendency to exhibit monolayer smectic phases and the driving force for their formation is the incompatibility between the terminal alkyl chains and the spacers, leading to a microphase separation into three regions: terminal chains, mesogenic groups and flexible alkyl spacers [3].

In contrast, non-symmetric liquid crystal dimers often exhibit intercalated smectic phases, in which specific molecular interactions between the two different mesogenic units account for this specific phase behavior [1–3, 7, 8]. The question arises, what would happen if the interaction between the identical mesogenic units in symmetric dimers increases? To investigate this, we have designed a series of symmetric liquid crystal dimers containing a hydrazide group as the mesogenic units (see scheme 1), in which lateral intermolecular hydrogen bonding was expected to increase the intermolecular interaction. Nitro, phenyl, and methyl terminal groups, instead of long alkyl chains, were used as terminal substituents to avoid the unfavourable interaction between the terminal alkyl chains and spacers [2, 3].

This study was stimulated by recent work in which we have demonstrated that lateral intermolecular hydrogen bonding was still interacting in the SmA phase and played an important role in stabilizing the mesophase of dissymmetric hydrazide derivatives [9], as shown in scheme 1, which can be regarded as the monomeric analogues of the present dimers. It has been demonstrated that intermolecular hydrogen bonding plays an important role in mesophase formation in the hydrazide derivatives; for example, linear *N*,*N*′-bis(4-alkoxybenzoyl)hydrazines

---

*Corresponding author. Email: minli@mail.jlu.edu.cn

ISSN 0267-8292 print/ISSN 1366-5855 online
http://www.tandf.co.uk/journals
DOI: 10.1080/02678290600604841

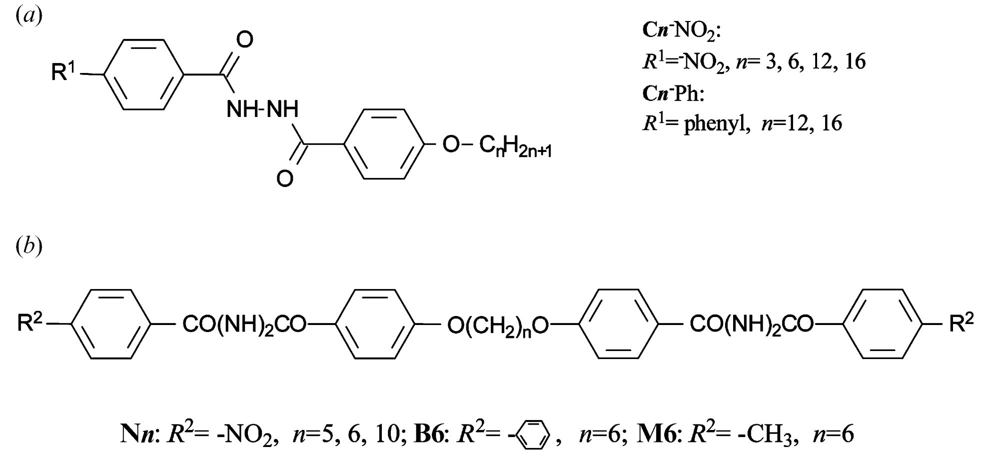

Scheme 1. The molecular structures of (*a*) monomeric and (*b*) dimeric hydrazide derivatives.

exhibit a cubic phase [10–12], while monomeric, dimeric and polymeric *N*,*N*′-bis[3,4,5-tris(alkoxybenzoyl)]hydrazines form a columnar phase [12, 13]. Here, we report the synthesis, phase behaviour and mesophase structures of α,ω-bis[*N*-(4-nitrobenzoyl)-*N*′-(benzoyl-4′-oxy)hydrazine]alkanes (**N*n***, ***n*** indicating the number of carbon atoms in the spacer), 1,6-bis[*N*-(4-biphenylcarbonyl)-*N*′-(benzoyl-4′-oxy)hydrazine]hexane (**B6**), and 1,6-bis[*N*-(4-methylbenzoyl)-*N*′-(benzoyl-4′-oxy)hydrazine]hexane (**M6**).

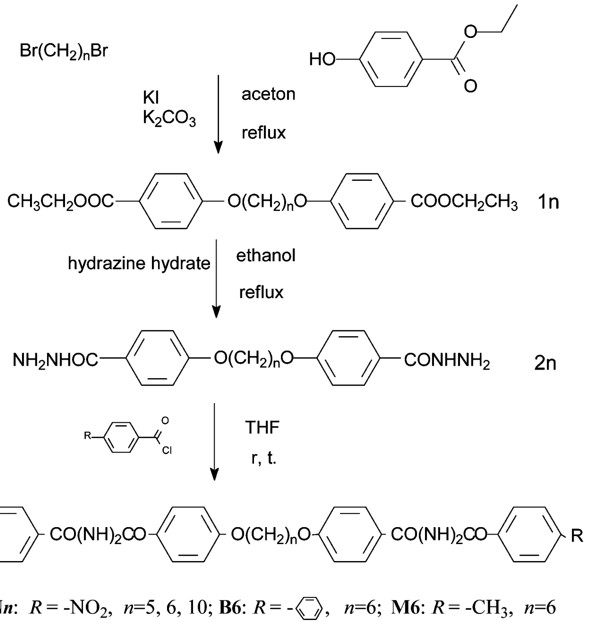

Scheme 2. The synthesis of **N*n***, **B6**, and **M6**.

2. Experimental

2.1. *Synthesis*

N*n*, **B6** and **M6** were synthesized by the route shown in scheme 2. Firstly, α,ω-bis[4-(ethylbenzoate)-1-oxy]alkane (**1*n***) was synthesized by a Williamson etherification [14]. Secondly, **1*n*** reacted with excess hydrazine hydrate in ethanol to give α,ω-bis(4-hydrazinylbenzoyl-1-oxy)-alkane (**2*n***) [14, 15]. Finally, the target products were obtained through the reaction of **2*n*** and the corresponding benzoyl chloride in tetrahydrofuran at room temperature. A small amount of pyridine as catalyst was added to the reaction mixture. All the compounds were purified by recrystallization from a mixture of DMSO and ethanol for further ^{1}H NMR measurements and elemental analysis; yield>80%.

2.1.1. 1,6-Bis[*N*-(4-nitrobenzoyl)-*N*′-(benzoyl-4′-oxy) hydrazine]hexane (N6).

^{1}H NMR (500 MHz, DMSO), (ppm, from TMS): 10.79 (s, 2H); 10.46 (s, 2H); 8.38 (d, 4H, J=8.8 Hz); 8.14 (d, 4H, J=8.8 Hz); 7.90 (d, 4H, J=8.8 Hz); 7.06 (d, 4H, J=8.8 Hz); 4.08 (t, 4H, J=6.4 Hz); 1.78 (m, 4H); 1.51 (s, 4H). Anal: calcd for $C_{34}H_{32}N_6O_{10}$, C 59.65, H 4.71, N 12.27; found, C 59.69, H 4.67, N 12.33%.

2.1.2. 1,6-Bis[*N*-(4-biphenylcarbonyl)-*N*′-(benzoyl-4′-oxy)hydrazine]hexane (B6).

^{1}H NMR (500 MHz, DMSO), (ppm, from TMS): 10.49 (s, 2H); 10.36 (s, 2H); 8.02 (d, 4H, J=8.4 Hz); 7.92 (d, 4H, J=8.8 Hz); 7.83 (d, 4H, J=8.4 Hz); 7.76 (d, 4H, J=7.3 Hz); 7.51 (t, 4H, J=7.6 Hz); 7.43 (t, 2H, J=7.3 Hz); 7.06 (d, 4H, J=8.8 Hz); 4.08 (t, 4H, J=6.4 Hz); 1.79 (m, 4H); 1.52 (s, 4H). Anal: calcd for $C_{46}H_{42}N_4O_6$, C 73.98, H 5.67, N 7.50; found, C 73.88, H 5.30, N 7.10%.

2.1.3. 1,6-Bis[*N*-(4-methylbenzoyl)-*N*′-(benzoyl-4′-oxy) hydrazine]hexane (M6). ^{1}H NMR (500 MHz, DMSO), (ppm, from TMS): 10.34 (s, 2H); 10.29 (s, 2H); 7.89 (d, 4H, J=8.7 Hz); 7.82 (d, 4H, J=8.1 Hz); 7.32 (d, 4H, J=8.0 Hz); 7.04 (d, 4H, J=8.8 Hz); 4.07 (t, 4H, J=6.4 Hz); 2.38 (s, 6H); 1.78 (m, 4H); 1.51 (s, 4H). Anal: calcd for $C_{36}H_{38}N_4O_6$, C 69.44, H 6.15, N 9.00; found, C 69.70, H 6.20, N 8.78%.

2.2. *Characterization*

^{1}H NMR spectra were recorded with a Bruker Avance 500 MHz spectrometer, using DMSO-d6 as solvent and tetramethylsilane (TMS) as an internal standard. Phase transitional properties were investigated with a Netzsch DSC 204. Texture observation was conducted on a Leica DMLP polarizing optical microscope equipped with a Leitz 350 microscope heating stage. X-ray diffraction was carried out with a Bruker Avance D8 X-ray diffractometer.

3. Results and discussion

3.1. *Phase behaviors of N*n*, M6, and B6*

The phase behaviours of **N*n***, **M6** and **B6** were studied by polarizing optical microscopy (POM), differential scanning calorimetry (DSC), and wide-angle X-ray diffraction (XRD). All three compounds **N*n*** (n=5, 6, 10) showed fan-shaped texture in both heating and cooling runs, as showed in figures 1 (*a–c*), indicating smectic behaviour. We noticed that the fan-shaped texture of **N10**, figure 1 (*c*), remained unchanged if the film was cooled to room temperature at 10°C min^{-1}. Crystalline regions in coexistence with a fan-shaped texture developed if the film of **N10** was kept isothermally at 200°C for about 30 min. Similar behaviour was found in **N6**. These observations indicate that crystallization of **N10** and **N6** from their molten state is difficult, which was also confirmed by DSC and XRD. In the DSC measurements, a large and broad exothermic peak appeared, when compound **N10** was

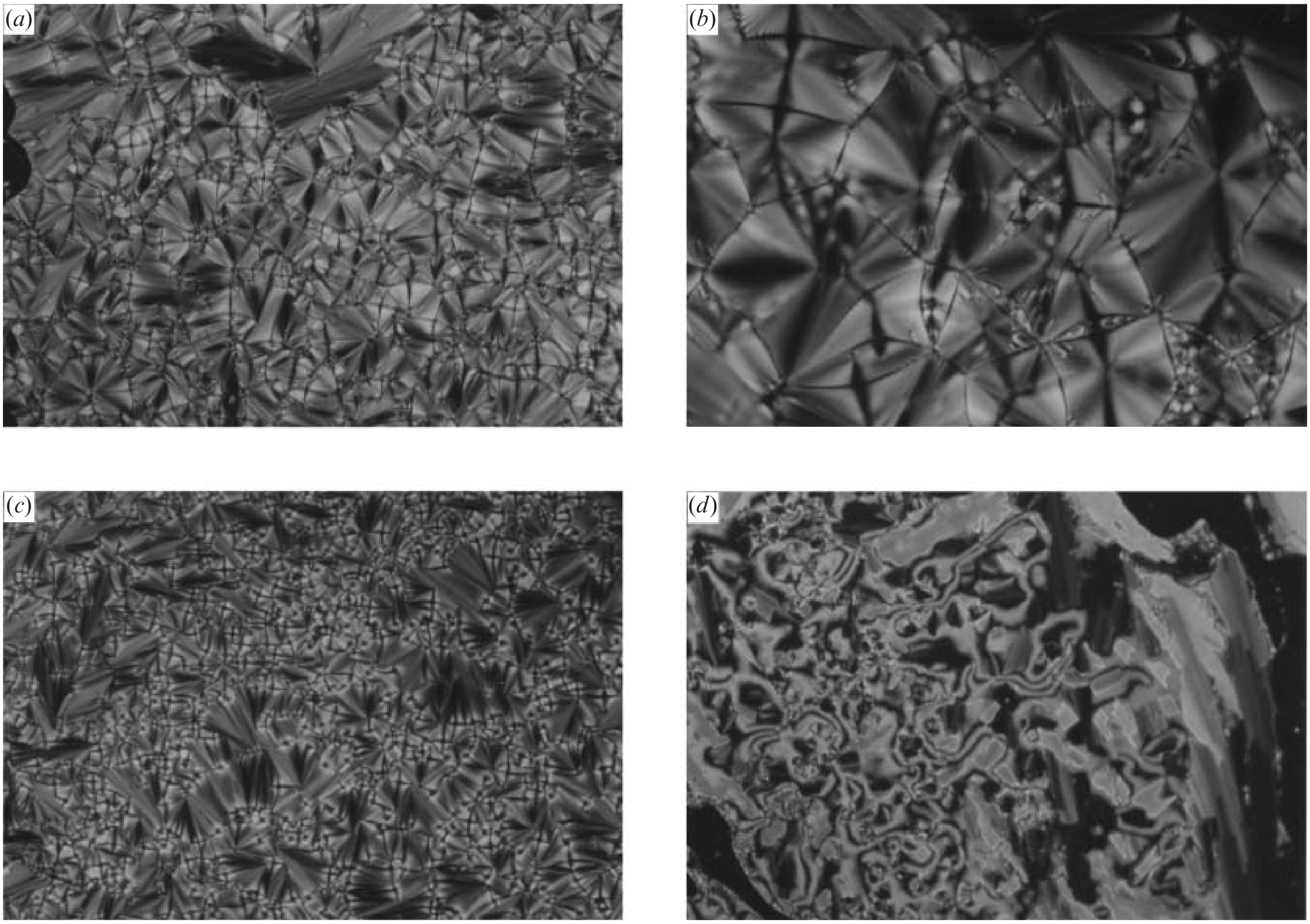

Figure 1. Polarizing optical photomicrograph of **N*n*** and **B6**. (*a*) fan-shaped texture of N5 at 273 (× 200); (*b*) fan-shaped texture of N6 at 290 (× 400); (*c*) fan-shaped texture of N10 at 20 (× 200); (*d*) the coexisting of Scheliren and fan-shaped texture of B6 at 300 (× 200).

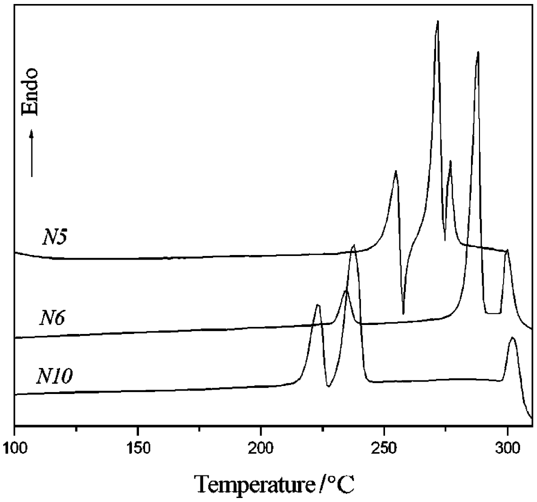

Figure 2. DSC curves of **N*n*** in the first heating run.

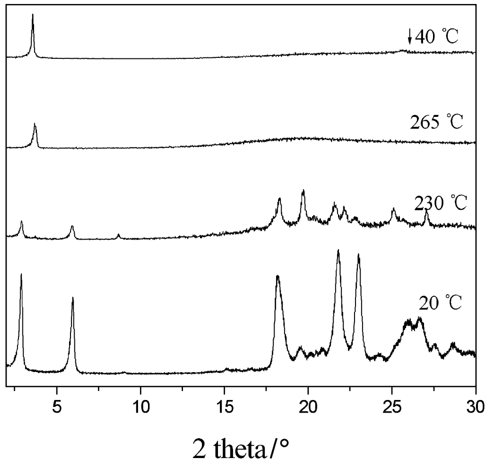

Figure 3. X-ray diffraction pattern of **N10** at different temperatures.

cooled from the mesophase, confirming crystallization. However, only one sharp diffraction peak in the low angle region, as well as some very weak crystallization peaks could be found in the XRD pattern of **N10** taken at 20°C during cooling, indicating that the compound did not crystallize easily. The natural texture of **B6** contains both the Schlieren and fan-shaped textures, as shown in figure 1 (*d*), which changed to a full Schlieren texture upon shearing, indicating nematic behaviour of B6 [16]. The compound **M6** is non-mesomorphic.

The compounds of **N*n*** series degraded just above the isotropic transition temperature, as evidenced by DSC, see figure 2. So phase transitional temperatures are based on the results of the first heating run. The compounds **N*n*** (n=5, 6, 10) exhibited similar phase sequence, Cr_1–Cr_2–Sm–I (see figure 2), except that **N5** showed an exothermic peak at 257.3°C, which is associated with the crystallization of the sample. The polymorphic behaviour was confirmed by X-ray diffraction (XRD); for example, figure 3 shows the XRD patterns of **N10** in the crystalline state (at 20 and 230°C) and the mesophase (at 265°C). It is apparent that the crystal structure changes during the transition from Cr_1 to Cr_2.

Table 1 gives the phase transition temperatures and associated enthalpy changes. The odd–even effect, which is characteristic of liquid crystal dimers [2], was observed in compounds **N5** and **N6**; both the melting and clearing points of **N5** are much lower than those of **N6**. Compared with that of **N6**, the melting point of **N10** decreased, and its clearing point increased, with the increase in length of the spacer, indicating that the mesophase can be stabilized by its elongation. The terminal substituents also played an important role in the formation and stabilization of the mesophase. The exhibited mesomorphic behaviour of **B6** and **N*n*** indicated that the rigid substituents and introduction of a dipole along the molecular long axis favoured the formation of a mesophase. The non-mesomorphic behaviour of **M6** is not due to its higher melting point; indeed **M6** exhibits the lowest melting point among them, indicating that the shape anisotropy or dipolar interaction is required for the mesophase.

Table 1. Phase behaviour of **N*n***, **B6** and **M6**.

Compound	Cr_1	T/°C	Cr_2	T/°C (ΔH/kJ mol^{-1})	Meso	T/°C (ΔH/kJ mol^{-1})	I
N5	•	254.9	•	271.5(52.70)	•	276.5(13.44)	•
N6	•	234.5	•	287.5(75.18)	•	299.7(—)^a	—
N10	•	223.3	•	237.5(68.68)	•	301.9(—)^a	—
B6	•	241.4	•	298.4(91.64)	•	307.4(6.22)	•
M6	•	—	—	258.5(113.77)	—	—	•

[a] **N6** and **N10** degrade near the isotropic transition. [b] Cr, Meso, and I indicate crystalline state, mesophase, and isotropic liquid, respectively.

3.2. *Mesophase structure of B6 and N*n

In order to obtain further information on molecular arrangements in their mesophase, variable temperature XRD was performed on **B6** and **N*n***. A characteristic pattern of the nematic phase was observed in the mesophase of **B6**. Interestingly, apart from the diffuse peak centred at a spacing of 4.6 Å, typical for molten alkyl chains, another diffuse peak located at a spacing of 21.1 Å, which was about half the molecular length (43.8 Å), was observed at the lower angle region, indicating that the molecules of **B6** are intercalated in the nematic phase to form a more or less layered structure similar to that in the $\mathrm{SmA_c}$ phase. It agrees well with the observation that a fan-shaped texture co-existed with the schlieren texture, as described above.

The XRD pattern of **N10** in the smectic phase contains a single sharp peak in the low angle region implying the formation of a layered structure, and a broad diffuse peak in the wide angle region centred at a spacing of 4.6 Å, indicating liquid-like arrangement of the molecules within the layers. The layer spacing (d) is 23.6 Å, which is comparable to one half of the estimated all-*trans* molecular length (l), of the most extended conformation of 42.8 Å, indicating that the molecules of **N10** are arranged in an intercalated layered structure, termed $\mathrm{SmA_c}$, in which different parts of the molecules, terminal substituents, spacers, and mesogenic moieties, overlap [2, 3]. Similar molecular arrangements were observed for compound **N5** and **N6**; data for d, l and d/l ratios are collected in table 2.

An intercalated smectic phase has generally been observed in non-symmetric liquid crystal dimers, and was thought to be stabilized by an electrostatic quadrupolar interaction between different mesogenic groups having quadrupole moments of opposite sign. Only a few exceptional examples have been reported, such as in the series of α,ω-bis (4,4′-butoxybiphenylcarbonyloxy)alkanes reported by Watanabe and Komura [17]. Even-membered homologues of this series exhibit the intercalated smectic A phase, while the odd-membered form the intercalated smectic C phase. It is not clear why these dimers exhibit intercalated phases although it has been suggested that a specific dipolar interaction may exist between the ester groups of the spacers and the ether groups of the terminal chains, which might offset the apparently unfavourable interaction between the spacers and the terminal chains.

Table 2. Summary of X-ray diffraction results for **N*n*** in the mesophase.

Compound	Molecular length[a] l/Å	T/°C	Layer spacing d/Å	d/l
N5	36.0	272	19.8	0.55
N6	37.7	290	20.7	0.54
N10	42.8	265	23.6	0.55

[a]Molecular length was calculated by AM1.

In the present study, symmetric liquid crystal dimers without terminal alkyl chains have been designed, in which the unfavourable interaction between the spacer and the terminal chains is avoided. Additionally, lateral intermolecular hydrogen bonding between the hydrazide groups, as has been confirmed in the monomeric series [9], might be the origin of a special interaction, similar to that in non-symmetric dimers in which a strong interaction between different mesogenic moieties exists, driving the formation of the intercalated phase. Unfortunately, the high mesophase transition temperature of the dimers precluded their study by infrared spectroscopy.

4. Conclusion

An intercalated smectic phase has generally been observed in non-symmetric liquid crystal dimers, and was thought to be driven by a special interaction between the different mesogenic moieties. In the present study, we have introduced intermolecular hydrogen bonding into symmetric liquid crystal dimers, by choosing the hydrazide group in the mesogenic units; and intercalated smectic phases in these symmetric dimers were observed. Based on the results of our previous work on monomeric hydrazide derivatives, intermolecular hydrogen bonding between the identical mesogenic units is considered to drive the formation of the intercalated structures. However, the interaction between terminal alkyl chain and the spacer has been omitted in the present study, and will be included in future work.

Acknowledgements

The authors are grateful to the National Science Foundation Committee of China (project No. 50373016), Program for New Century Excellent Talents in Universities of China Ministry of Education, Special Foundation for PhD Program in Universities of China, Ministry of Education (Project No. 20050183057), and Project 985-Automotive Engineering of Jilin University for their financial support of this work.

References

[1] C.T. Imrie, G.R. Luckhurst. *Handbook of Liquid Crystals*, Vol. 2B, D. Demus, J.W. Goodby, G.W. Gray, H.W. Spiess, V. Vill (Eds), p. 801, Wiley-VCH, Weinheim (1998).

[2] C.T. Imrie. *Struct. Bond.*, **95**, 149 (1999).

[3] C.T. Imrie, P.A. Henderson. *Curr. Opin. colloid. inter. Sci.*, **7**, 298 (2002).

[4] A.C. Griffin, T.R. Britt. *J. Am. chem. Soc.*, **103**, 4957 (1981).

[5] G.R. Luckhurst. *Macromol. Symp.*, **96**, 1 (1995).

[6] R.W. Date, C.T. Imrie, G.R. Luckhurst, J.M. Seddon. *Liq. Cryst.*, **12**, 203 (1992).

[7] J.L. Hogan, C.T. Imrie, G.R. Luckhurst. *Liq. Cryst.*, **3**, 645 (1988).

[8] G.S. Attard, R.W. Date, C.T. Imrie, G.R. Luckhurst, S.J. Roskilly, J.M. Seddon, L. Taylor. *Liq. Cryst.*, **16**, 529 (1994).

[9] D.M. Pang, H.T. Wang, M. Li. *Tetrahedron*, **61**, 6108 (2005).

[10] D. Demus, A. Gloza, H. Hauser, I. Rapthel, A. Wiegeleben. *Cryst. Res. Technol*, **16**, 1445 (1981).

[11] S. Kutsumizu. *Curr. Opin. solid state mater. Sci.*, **6**, 537 (2002).

[12] U. Beginn. *Prog. polym. Sci.*, **28**, 1049 (2003).

[13] U. Beginn, G. Lattermann, R. Festag, J.H. Wendorff. *Acta. Polym.*, **47**, 214 (1996).

[14] M. Li, C.W. Guo, Y.Q. Wu. *Liq. Cryst.*, **29**, 1031 (2002).

[15] B.L. Bai, M. Li, D.M. Pang, Y.Q. Wu, H.H. Zhang. *Liq. Cryst.*, **32**, 755 (2005).

[16] C.T. Imrie, P.A. Henderson, J.M. Seddon. *J. mater. Chem.*, **14**, 2486 (2004).

[17] J. Watanabe, H. Komura, T. Niiori. *Liq. Cryst.*, **13**, 455 (1993).